Effects of Alkali Metal Halide Salts on the Hydrogen Bond Network of Liquid Water

Christopher D. Cappa, Jared D. Smith, Kevin R. Wilson, Benjamin M. Messer, Mary K. Gilles, Ronald C. Cohen, and Richard J. Saykally*

Department of Chemistry, University of California and Chemical Sciences Division, Lawrence Berkeley National Laboratory, Berkeley, California 94720-1460

Received: December 1, 2004; In Final Form: February 7, 2005

Measurements of the oxygen K-edge X-ray absorption spectrum (XAS) of aqueous sodium halide solutions demonstrate that ions significantly perturb the electronic structure of adjacent water molecules. The addition of halide salts to water engenders an increase in the preedge intensity and a decrease in the postedge intensity of the XAS, analogous to those observed when increasing the temperature of pure water. The main-edge feature exhibits unique behavior and becomes more intense when salt is added. Density functional theory calculations of the XAS indicate that the observed *red shift* of the water transitions as a function of salt concentration arises from a strong, direct perturbation of the unoccupied molecular orbitals on water by anions, and does not require significant distortion of the hydrogen bond network beyond the first solvation shell. This contrasts the temperature-dependent spectral variations, which result primarily from *intensity* changes of specific transitions due to geometric rearrangement of the hydrogen bond network.

Introduction

The evolution of molecular geometric and electronic structure during ionic solvation by liquid water is fundamental to understanding the behavior of ions in chemical and biological systems and processes. It is generally thought that the presence of ions can either enhance or weaken the local hydrogen bond network, depending on the ionic charge and size, but quantification of these effects and their fundamental causes is difficult. X-ray diffraction and neutron scattering studies provide information on the local atomic arrangement of water molecules around an ion, demonstrating, for example, that both the $X^- - O$ and $Y^+ - O$ distances increase with increasing ionic radius in the alkali metal halide series (X^- = halide anion, Y^+ = cation), and that waters preferentially orient with a single hydrogen directed toward an anion, but with the hydrogens directed away from a cation.[1] The effect of ions on the HH pair correlation function has been interpreted as an increase in the "equivalent pressure" of the solution, although the changes are also generally consistent with an increase in temperature (e.g., there is a decrease in orientational correlations upon salt addition).[2]

IR vibrational femtosecond pump/probe experiments on aqueous halide solutions suggest that the vibrational lifetime is 2−4 times longer for water molecules directly hydrogen bonded with the halide ions than for water molecules hydrogen bonded with other water molecules.[3] The vibrational lifetimes of these water molecules forming ion−water hydrogen bonds (HBs) depend on the halide identity, increasing from F^- to I^-.[3] Qualitatively, this is rationalized as a decrease in anharmonic coupling between the hydrogen bond and the intramolecular OH stretch, which is a result of a weakened hydrogen bond for the ion−water complex. Additionally, Raman spectroscopic studies demonstrate that, although changes in the shape of the vibrational bands with halide salt addition are anion independent, the per-molecule scattering intensity for water increases sharply with $I^- > Br^- > Cl^- > F^-$.[4] In general, the variation observed in the Raman spectrum with increasing salt concentration is

similar to that effected by heating water and does not result in any new features uniquely attributable to salt−water hydrogen bonds.

With a goal of developing a more detailed molecular understanding of anion hydration, small water/anion cluster systems have been studied using vibrational predissociation spectroscopy to elucidate the behavior of water molecules in direct contact with an anion.[5] In this experiment, the geometric and electronic structure of a water molecule is distorted in the strong electric field of the anion, which results in a red shift of the OH vibrational spectrum with a magnitude following the order $F^- \gg Cl^- > Br^- > I^-$. It was necessary to explicitly consider charge transfer from the anion to the water molecules in addition to electrostatic interactions used to describe the electronic structure of the halide−water HB.[6] For the smaller anions, a greater amount of charge is transferred from the anion onto the water molecule.[6] The strong perturbation induced by the ion on the local water electronic structure has consequences in larger halide/water clusters. For example, for $X^- \cdot (H_2O)_2$ with $X^- = Cl^-$, Br^-, or I^-, a water−water HB is formed, but when $X^- = F^-$ no such HB is formed.[5] However, with cluster sizes above ∼5 or 6 waters, the vibrational spectra rapidly broaden to resemble the bulk water vibrational spectrum, making it difficult to establish direct connections to the solvation environment of halide anions in bulk water. Also, for the larger halides (Cl^-, Br^-, and I^-), the anion is solvated asymmetrically by the water molecules (e.g., the halide is located on the surface of a water cluster),[7] which cannot be the case for bulk solvation.

Recently, the valence level electronic structures of liquid water and aqueous solutions have been probed using photoelectron spectroscopy.[8,9] The binding energies of the pure liquid water valence molecular orbitals are shifted to lower energies (∼1.5 eV) and significantly broadened when compared to the gas-phase transitions. Upon addition of halide salts, no significant changes are observed in the liquid water photoelectron spectrum. Hence, solvated anion valence orbitals have lower binding energies than anions in the gas phase; however, in

Effects of Alkali Metal Halides on H-Bonds in H₂O

J. Phys. Chem. B, Vol. 109, No. 15, 2005 **7047**

solution the perturbation of the valence level water orbitals by salt ions is minimal.

Here, we report the first systematic investigation of the near-edge X-ray absorption spectrum (XAS) of aqueous alkali metal halide solutions. XAS is an element-specific technique that provides information on the local electronic environment of atomic sites within molecules by probing the nature of the unoccupied orbitals. For water in particular, the electronic structure has been shown to be very sensitive to the specific hydrogen bonding configurations of the water molecules when probed by oxygen K-edge XAS.[10−15] By monitoring changes in the O K-edge spectrum, we directly probe changes induced by the halide salts in the local electronic structure of the unoccupied orbitals of the water molecules. This technique has recently been applied to transition metal ions in water, showing that new features are observed in the K-edge spectrum at low energies.[16] These new features are attributed to mixing between the molecular orbitals of water molecules and the open d-shell of the transition metal cation. The effects of salts on the major spectral regions of the liquid water XAS (i.e., the preedge, main edge, and postedge) have not been considered previously.

Methods

Experiment. The oxygen K-edge (∼535 eV) spectra for aqueous NaCl, NaBr, and NaI solutions were measured using a novel liquid microjet apparatus at Beamline 8.0.1 and Beamline 11.0.2 of the Advanced Light Source at Lawrence Berkeley National Laboratory. A detailed description of the experimental setup is presented in Wilson et al.[17] Briefly, tunable X-ray radiation is used to excite a 30 μm diameter liquid microjet target at normal incidence. Use of liquid microjets allows for windowless coupling to the high vacuum beamline through a differential pumping section as well as for charged particle detection. The pressure in the interaction chamber is typically ∼8 × 10⁻³ Pa, while the pressure in the beamline is maintained at <7 × 10⁻⁸ Pa. The liquid jet is in a horizontal configuration such that the polarization vector of the incident X-rays is parallel to the axis of propagation of the liquid jet. The liquid jet is formed by pressurizing the solutions behind 30 μm fused silica capillaries to ∼5 MPa using a quaternary low-pressure gradient HPLC pump, which allows for quick (∼5 min) and accurate (±1%) mixing to various salt concentrations. We have measured XAS spectra for 0.8, 2, 3, and 4 M aqueous solutions as well as for pure water.

The total electron yield (TEY) is collected on a biased copper electrode (+100 V) placed within 500 μm of the liquid jet/X-ray interaction region, orthogonal to both the X-ray beam and the liquid jet. The average escape depth of electrons from the liquid jet is sufficiently large that the TEY is a measure of the bulk liquid electronic structure.[18] The measured current is amplified and converted to a voltage for input to the beamline computer. All signals are normalized to I_0, which is measured simultaneously on a gold mesh located 3 m upstream from the interaction region. Recent improvements to the endstation allow for accurate and reproducible intersection of the liquid jet with the fixed X-ray beam. We have measured the full width at half-maximum (fwhm) of the overlap between the liquid jet and X-ray beam as 50 μm on Beamline 8.0.1 and 40 μm on Beamline 11.0.1, which implies an X-ray spot size of ∼10−20 μm in the vertical. The spot size in the horizontal is ∼150 μm. The monochromator slits were set to provide a nominal resolution of $E/\Delta E > 4000$ at 500 eV.

Computations. The XAS of liquid water and of aqueous salt solutions were calculated using the StoBe-DeMon 2.0 code.[19]

Initial calculations were performed using instantaneous configurations obtained from the output of a molecular dynamics (MD) simulation of SPC/E liquid water or 1.2 M NaX aqueous solutions (X = I⁻, Br⁻, or Cl⁻) at 300 K, where polarizations of both the solvent and the solvated ions are explicitly included.[20] By using a relatively large sampling of instantaneous configurations from the MD simulation, we are able to determine an average XAS for each halide system considered, explicitly considering variations in the hydrogen bonding environment about a given water molecule in the liquid.

Pure water XAS calculations were performed for 17 molecule clusters taken from the MD snapshot. For each calculation, a central molecule for which the spectrum is determined is selected, along with the 16 nearest neighbors based on their O−O distance. For pure water, a total of 44 randomly selected individual configurations were calculated. For the NaX$_{(aq)}$ systems, a central water molecule was selected from the six nearest neighbor water molecules to a given anion (or cation) based on the O−X⁻ (O−Y⁺) distance. Using each of these near-anion (near-cation) water molecules as the central molecule for the calculation, the 15 nearest neighbor waters were selected, as well as any Na⁺ or X⁻ molecules that were contained within the solvation shell defined by these 15 waters. Typically, half of the sampled configurations contain only one X⁻ molecule and half contain both a Na⁺ and an X⁻. For the near-cation calculations, only those configurations with a single Na⁺ were considered. For the salt cluster calculations a minimum of 20 individual spectra were calculated for each salt species.

As the StoBe-DeMon code does not calculate transition widths, the calculated transitions were broadened using a fwhm of 0.6 eV below 538 eV and 3 eV above 540 eV.[21] Between 538 and 540 eV the fwhm is linearly varied from 0.6 to 3 eV. All calculations were performed using the transition potential method under the half core hole approximation[22] using the nonlocal RPBE PBE functionals. For the 16 surrounding molecules, an effective core potential[23] was used to simplify the definition of the core hole and allow determination of the XAS spectrum of the central molecule. All calculated energies were shifted to lower energy by 1 eV for comparison with experiment.

We have also performed calculations on five-molecule clusters, wherein a central water molecule is surrounded by four other molecules in a nearly tetrahedral configuration (with respect to the oxygen atoms or anion/cation). This was done for $(H_2O)_5$, as well as for clusters where one of the waters is replaced by either a halide anion or a sodium cation (e.g., $(H_2O)_4X^-$). The cluster geometry was specified to have O−O (O−X⁻ or O−Na⁺) bond separations of 2.818 Å and O−H---O hydrogen bond angles of 175.9°. The anion position was selected such that it acted as a hydrogen bond acceptor from the central H_2O, whereas the cation replaced a hydrogen bond donor to the central H_2O.

Experimental Results

The oxygen K-edge XAS of liquid water has previously been shown to be a very sensitive probe of the specific hydrogen bonding configurations of the water molecules.[10−15] Here, we observe dramatic changes in the TEY XAS upon the addition of alkali metal halide salts to water. Each of the measured TEY signals has been normalized to I_0 and also area-normalized over the range 532−550 eV for comparison (Figure 1). The addition of a given sodium halide salt to water affects the O K-edge spectrum in qualitatively the same manner, independent of salt identity. There is a general increase in the intensity of the
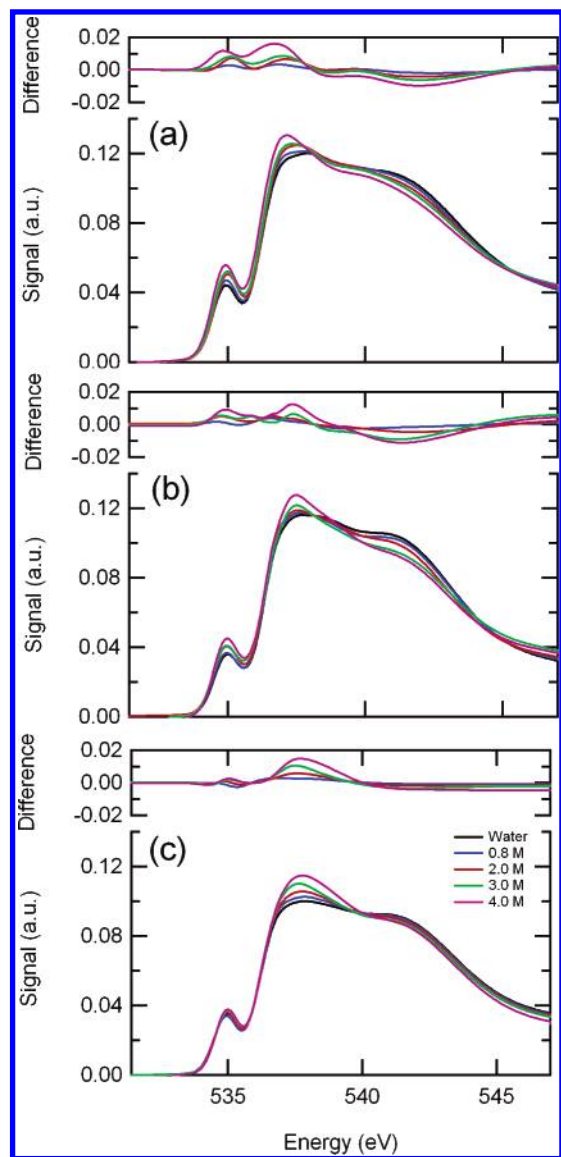
Figure 1. Evolution of O K-edge XAS of aqueous solutions as a function of concentration for addition of NaI (a), NaBr (b), and NaCl (c). All signals have been area normalized over the range 532−550 eV. The difference spectra between the aqueous salt solutions and pure water are shown for each halide solution considered.

preedge observed at 535 eV and of the main edge (~537.5 eV), with a concomitant decrease in the postedge (~541 eV).

Although there is a general decrease in the postedge feature for all salts, NaBr and NaI exhibit a high-energy isosbestic point (i.e., an energy where the normalized intensity is independent of salt concentration) at 544.4 and 545.7 eV (±0.2 eV), respectively, whereas no such point is observed for NaCl. A low-energy, salt-dependent isosbestic point is also observed on the main edge at 540.0, 538.4, and 537.9 eV (±0.4 eV) for NaCl, NaBr, and NaI, respectively. Furthermore, in the steeply rising region at ~536.5 eV, the NaI spectra exhibit a strong concentration-dependent red shifting, whereas only a small red shift is observed for NaBr solutions and no such shift is observed for NaCl solutions.

To further quantify these differences, the observed spectra were fit to six Gaussian peaks using linear least squares regression (see Figure 2). Six peaks was the minimum number found to give a reasonable fit to the XAS spectrum. The first five peaks are representative of the observed gas-phase features and the sixth is an approximate ionization step edge. For each
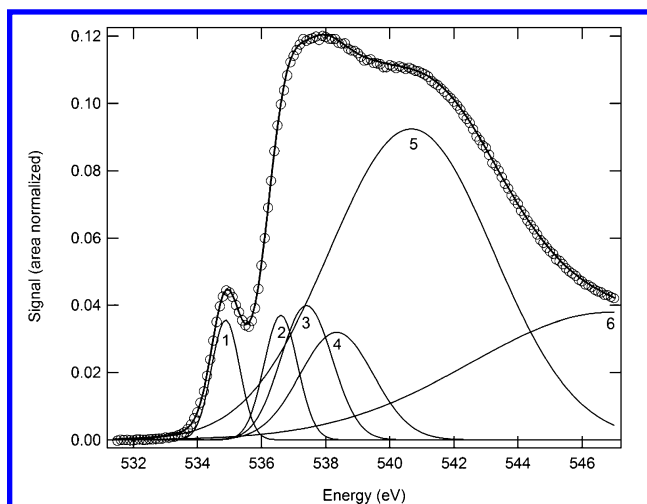

Figure 2. Observed oxygen K-edge XAS of pure water (O) fit to six Gaussians (solid line). The Gaussian parameters determined for pure water are used to fit the aqueous solution spectra (see text for details).

salt, a fit on the pure water spectrum for that data set provided the initial parameters for fitting of the aqueous salt spectra. The peak position of each of the Gaussian peaks is then locked, as are the peak height and width of peak 6. Subsequent fits to the aqueous salt solutions varied the height and width of each of the peaks. The main-edge feature is taken as the sum of the area of peaks 2, 3, and 4, while the postedge is taken as the area of peak 5 and the preedge is taken as the area of peak 1. It is observed that the preedge and main-edge features exhibit an approximately linear increase in area with salt concentration (by ~25% to 4 M, referenced to pure water, independent of the identity of the salt), whereas the postedge feature exhibits a moderate linear decrease in area (by ~10%) (Figure 3). Hence, the preedge/main-edge ratio is constant with added salt to within ~5%. In contrast, the preedge/postedge and main-edge/postedge ratios increase sharply with concentration, by ~40% to 4 M. We have recently confirmed that this linear variation persists to very high concentrations (~11 M LiCl).[24] Because six Gaussian peaks are used to fit the spectrum (resulting in a model with a high degree of flexibility), the above stated percent changes with added salt are only approximate. We have, however, assessed the overall validity of the trends characterized through our analysis method by generating initial fit parameters from different spectra, specifically by using the aqueous salt spectra to fix the center frequencies of the six Gaussians instead of the pure water spectrum. The general trends observed (i.e., the insensitivity of the preedge/main-edge ratio and the strong, near-linear increases of the preedge/postedge and main-edge/postedge ratios with salt concentration) are independent of the method for choosing the center frequencies.

Discussion

The spectral variations observed with salt addition indicate a strong perturbation of the electronic structure of water molecules in aqueous solutions. It is of interest to determine the origin of the specific changes observed in the different regions of the spectrum (i.e., the preedge, main edge, and postedge) and the isosbestic point observed. Our interpretation of these spectra is guided by XAS calculations on salt/water clusters. For example, in Figure 4 the average calculated XAS for pure water and aqueous solutions using configurations taken from the MD snapshots are shown. The *qualitative* changes observed in the water XAS upon addition of halide salts are reproduced in the average calculated spectrum, with a sharp
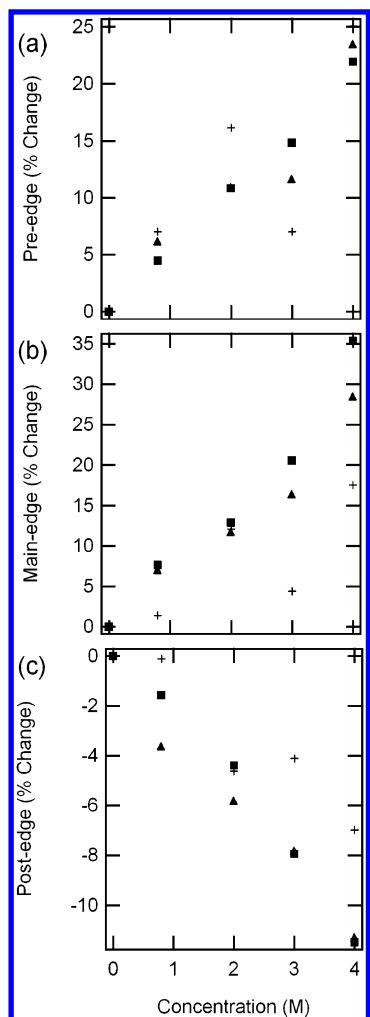
Figure 3. Variation of (a) preedge, (b) main-edge, and (c) postedge intensities of the O K-edge spectrum of liquid water with addition of NaCl (■), NaBr (+), and NaI (▲).

Figure 4. (top) Experimental and calculated XAS spectra of pure water using a sampling of 44 instantaneous configurations from an SPC/E simulation. (bottom) Calculated XAS spectra for pure water (black), $NaCl_{(aq)}$ solution (dark gray), $NaBr_{(aq)}$ solution (dashed), and $NaI_{(aq)}$ solution (light gray). Also shown is the calculated spectrum for $Na^+_{(aq)}$ solution (dotted).

increase of the main-edge feature and a concomitant decrease of the postedge feature. The bulk solution calculations, using these modest size clusters from MD snapshots, do not have the sensitivity to clearly establish the effect of the halide salt on the preedge feature. The criterion used to select water molecules from the 1.2 M $NaX_{(aq)}$ simulations (i.e., ion nearest neighbors) focuses primarily on the perturbative effect of the direct halide anion/water molecule interaction, and does not account for any orientation effects outside of the second solvation shell. Hence, the calculated average spectrum may seriously overestimate the effect of the salt at 1.2 M because we include in our calculations only water molecules that have a halide anion as a nearest neighbor. In fact, the effective molarity of the instantaneous configurations used in the calculations is ~6 M (i.e., there is one X^- in a box with ~6.5 Å sides), even though taken from a dilute MD simulation. Thus, it is not surprising that the calculated spectra exhibit changes more in accord with the observed high-concentration spectra.

The effect of the addition of a nearest neighbor Na^+ cation to the water XAS has also been considered explicitly (Figure 4). It is clear that the perturbative effects of a Na^+ ion in a hydrogen bond "donor" position, with respect to the central water molecule, are smaller than those of a halide anion in an "acceptor" position, although they are still significant. In particular, there is an overall increase of the preedge intensity and a small decrease in both the main edge and postedge. Similar to the effects of halides, the main edge does exhibit a slight
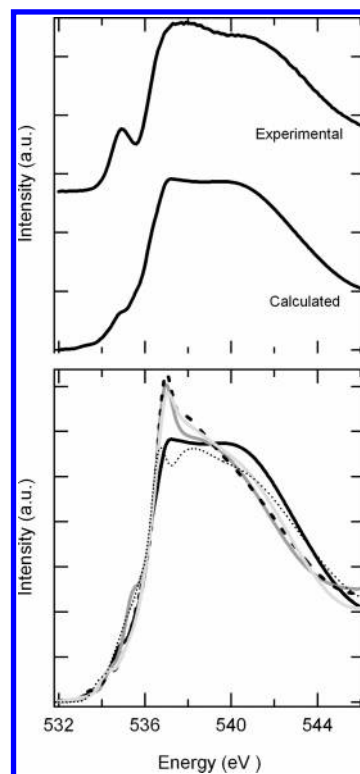
narrowing upon addition of the Na^+. Future studies to understand the effect of cations on the XAS are clearly warranted.

The above calculations help to characterize the overall effect of addition of a halide species on the water XAS. However, from these results, we cannot directly distinguish between the effect of the salt on the local water geometric structure and the perturbation of the anion on the electronic structure of its near-neighbor water molecules. To address this, the XAS of model tetrahedral water pentamers, where one hydrogen bond acceptor molecule is replaced with a halide anion, have been calculated (Figure 5). As a first approximation the $O-X^-$ or $O-Na^+$ distance is fixed at the $O-O$ water pentamer value (2.8 Å). Replacing a water molecule with an X^- in a hydrogen bond acceptor position results in a decrease in the postedge intensity and an increase and a narrowing of the main-edge region (Figure 5). This effect increases with increasing anion size ($Cl^- < Br^- < I^-$).

The calculated stick spectrum indicates that the intensity at the main edge for the pure water pentamer arises primarily from a single strong transition. In contrast, the increase in the main-edge intensity for the halide/water pentamers results from an increase in the number of transitions at the main edge, rather than to any marked increase in oscillator strength of a given transition at this energy (Figure 5). Similarly, the observed loss of postedge intensity results from a decrease in the number of transitions in this region by more than a factor of 2 compared to pure water. When the transition density is considered over a larger energy region (e.g., up to 545 eV), the total number of calculated transitions is nearly identical for the pure water and halide/water pentamers. As such, we associate changes observed in the main edge and postedge with a *shifting* of allowed transitions to lower energies upon halide addition. This is shown
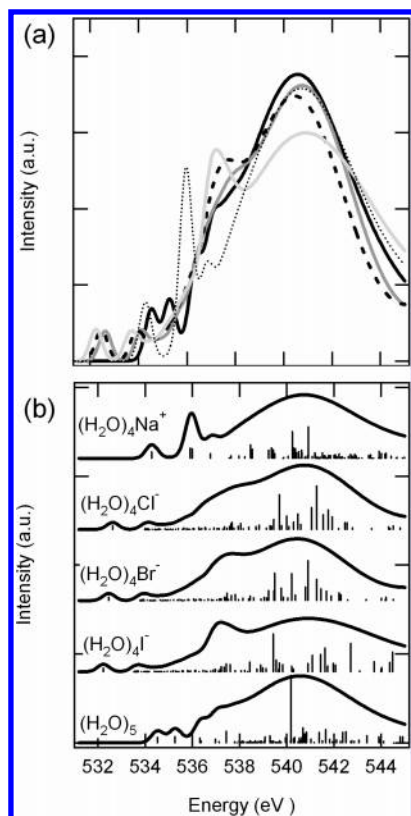
Figure 5. (a) Calculated XAS of the central molecule in a tetrahedral water pentamer (solid black). Calculated XAS are also shown for replacing one of the hydrogen bond acceptor water molecules with a halide anion for Cl^- (dark gray), Br^- (dashed), and I^- (light gray). Also shown is the effect of replacing a hydrogen bond donor water with a sodium cation (dotted). (b) Calculated XAS spectra from (a) with associated stick spectra.
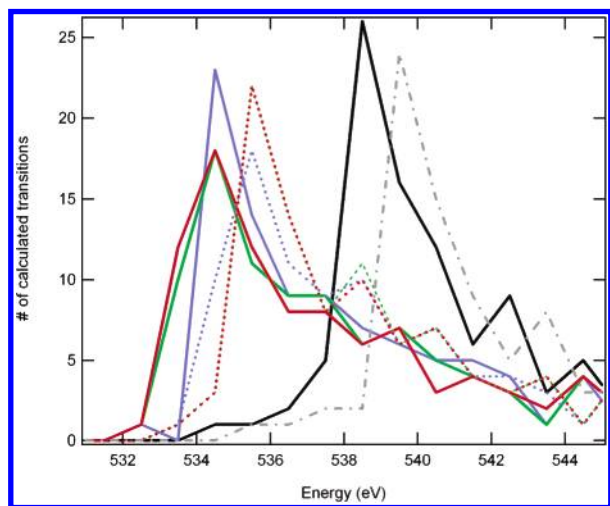

Figure 6. Calculated transition density in 1 eV bins for the water pentamer (black), $(H_2O)_4Cl^-$ (blue), $(H_2O)_4Br^-$ (green), and $(H_2O)_4I^-$ (red). The solid lines are for the fixed geometry pentamers (see Figure 5), and the dashed lines are for when explicit $O-X^-$ distances have been considered (see Figure 7). Shown for comparison is the single donor water tetramer (gray, dot–dashed).

explicitly by counting the calculated number of transitions in 1 eV bins for the pure water and halide–water pentamers (Figure 6). This finding is consistent with the experimental observation of an (halide-dependent) isosbestic point at ∼539 eV, between the main edge and postedge. The experimental isosbestic point is observed at the lowest energy for the case of I^- addition, suggesting that I^- engenders a stronger perturbation and red

shift of the oxygen K-edge transitions. This occurs despite the fact that for halide solutions the oxygen–halide distance is experimentally observed to follow the order $R(O-I^-) > R(O-Br^-) > R(O-Cl^-)$.[25] In the calculated orbital contour diagrams (not shown) the asymmetric electronic environment of the ion–water clusters results in localization of the electron density along the OH bond of the central water pointed away from the anion.

Moreover, the small preedge feature observed at ∼535 eV in the water pentamer spectrum is red shifted by ∼2 eV and is split upon exchange of a water with an X^-. The magnitude of the shift (but not the splitting) depends on anion size. Experimentally, no new features were observed at low energy, suggesting that the perturbation introduced on the preedge orbitals is relatively small, a result that is inconsistent with our calculations. However, as with the calculations utilizing larger clusters obtained from MD simulations above, we find that accurate calculation of these low energy features is problematic in these small model systems, possibly due to the formation of artificial surface states that give rise to low energy features.[26] In particular, for the pentamer system, we have not considered possible geometric distortion of water–water hydrogen bonds due to the anion and we also neglect long-range effects on the electronic structure. In light of this, sensitivity tests on water clusters of various sizes were performed. Although the exact details of the calculation do depend importantly on cluster size, the general shape of the calculated spectrum can be approximated as independent of cluster size. This result is in agreement with recent work on pure water clusters, demonstrating that complete convergence of the calculated XAS spectrum is not obtained even up to clusters of 50 molecules.[26] We have found that the calculated salt solution spectra have an even stronger dependence upon cluster size for the lower energy transitions (i.e., in the preedge region), making a unique interpretation of those features difficult. Therefore, we conclude that although these calculations, performed using small, model clusters (either artificially generated or taken from MD simulations), can be used to *qualitatively* rationalize the experimentally observed changes above the preedge, quantitative agreement is not to be expected.

We have also considered the effect of placing the halide anions at their experimentally determined $O-X^-$ distances, with $R(O-Cl^-) = 3.15$ Å, $R(O-Br^-) = 3.35$ Å, and $R(O-I^-) = 3.6$ Å.[25] Using these values, the calculated XAS exhibit smaller variations upon replacement of a water molecule with a halide ion in the pentamer system (Figure 7). A clear transfer of intensity from the postedge to the main edge is still evident, with the magnitude of this shift following the trend $I^- \sim Br^- > Cl^-$, consistent with the experimentally observed spectral variation. As an example, the total number of calculated transitions from low energy up to 538 eV for the water pentamer is 10, whereas for the iodide pentamer it is nearly 50 (see Figure 6). As above, the total number of calculated transitions over a larger energy range is conserved. Thus, we find that, even when the $R(O-X^-)$ differences are taken into account, I^- still produces larger changes in the calculated XAS spectrum than Cl^-, and that these changes result from a general shift of the calculated transitions to lower energies, compared to the pure water pentamer.

Upon exchanging a *donor* water molecule with Na^+, very different effects are observed (Figure 5). First, the behavior of the preedge features is quite different compared to that of the anion–water clusters, with a small blue shift and strong increase in intensity of one of the observed features (although this may again be a result of using small clusters). Furthermore, the
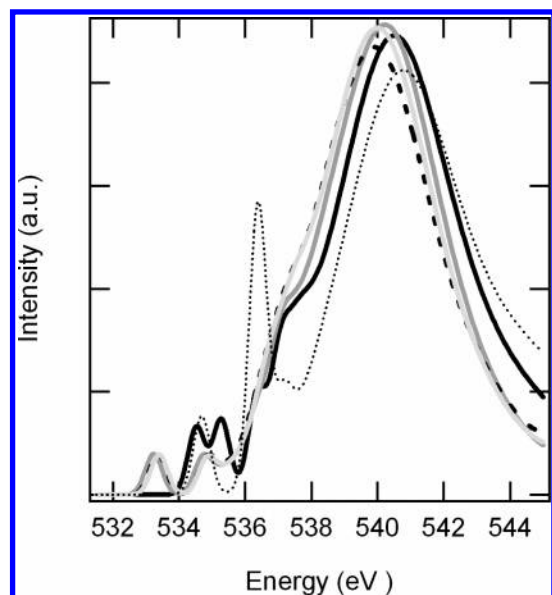
Figure 7. Calculated XAS for tetrahedral pentamer clusters, where differences in $R(O-X^-)$ for the different anions are explicitly considered (see text for details). Line colors are the same as in Figure 5.

intensity at the main edge is greatly decreased for the (H$_2$O)$_4$-Na$^+$ pentamer system, in contrast to the larger cluster calculations discussed above and to the effect of anions. Examining the (H$_2$O)$_4$Na$^+$ XAS stick spectrum, we identify the loss in main-edge intensity with a blue shift of the calculated transitions—the opposite behavior of the (H$_2$O)$_4$X$^-$ clusters. Nonetheless, this result is striking because the sodium cation interacts with a water molecule on the HB acceptor side of the central water. Results for pure water clusters suggest that molecules on the acceptor side have only a minimal effect on the observed XAS spectrum and that variations in the donating hydrogen bonds have the greatest effect.[12,13] This suggests that, as a water molecule solvates a cation, the cation influences the electronic structure of the surrounding water molecules and that distortions on the acceptor side may be considerably more important than previously thought. There may therefore be a distinct cation dependence on the O K-edge XAS water spectrum.

In recent studies of the temperature dependence of the liquid water XAS spectrum, spectral changes associated with temperature changes have been interpreted as arising from minor geometric distortions of the H-bonds.[10] The observed temperature-induced spectral intensity changes occurred only in the preedge and postedge regions; the main-edge spectral intensity was nearly independent of temperature, in contrast to the salt-induced changes. As temperature increases, strongly hydrogen bonded (tetrahedrally coordinated "ice-like") molecules rearrange to more weakly bonded configurations, as evidenced by an increase in the preedge/postedge ratio. No temperature-dependent isosbestic point was observed, although we note that X-ray Raman studies of liquid water at high temperatures provide some evidence for a temperature-dependent isosbestic point.[27] Thus, we find that variations in the O K-edge XAS due to salt addition or temperature change are manifested in different ways. We have shown that the presence of salt ions perturbs the vacant orbitals of the near-neighbor water molecules to such an extent as to lead to a redistribution of the water spectral transitions to lower energy. This is indicated by the large increase in main-edge intensity and the observation of isosbestic points between the main and postedge, both of which are not observed with temperature changes. The absence of a temperature-dependent isosbestic point suggests that a different

process determines the observed spectral variation. We suggest instead that structural changes induced by changing temperature lead primarily to variations in *spectral intensity* of specific transitions, and only to minor energy shifts of the transition energies. The calculated single donor water tetramer XAS demonstrates that redistribution of orbitals to lower energies upon "breaking" a water−water HB is minor compared to formation of an anion−water HB (Figure 6). Thus, spectral changes arising from geometric distortion of the HB network are more associated with changes in *oscillator strength* of specific transitions. The sensitivity of the preedge/postedge ratio to temperature is thought to arise from rehybridization of the water orbitals to have greater O p character upon distortion of the symmetric, tetrahedral bond configuration. The difference between salt addition and temperature changes is observed because the addition of salt not only breaks this symmetry, but more importantly leads to a strong, direct perturbation of the electronic structure of the surrounding water molecules through electrostatic interactions, whereas for temperature changes the spectral variation is strictly due to electronic changes arising from geometric rearrangement of the hydrogen bond network.

We note also the difference in behavior of the valence level orbitals (as probed by photoelectron spectroscopy[9]) vs the unoccupied orbitals (as probed by core level XAS) upon salt addition. The photoelectron spectra of pure liquid water and aqueous solutions were indistinguishable. This insensitivity of the valence level electronic structure to the presence of salt ions is in direct contrast to the strong perturbations on the unoccupied water orbitals observed in this work. Thus, solvated anion−water interactions appear to be primarily determined by interactions between the anion and the *unoccupied* orbitals on water molecules. One possible explanation for this difference is that the spatial extent of the unoccupied water orbitals is greater than for the valence level orbitals. As such, greater overlap of the unoccupied water orbitals with the hydrogen bound anion is likely, compared to the more localized valence orbitals.

That the preedge and main-edge/postedge ratios vary nearly linearly with salt concentration up to high [NaX] is striking. At low concentrations, one might expect that each water molecule is effectively isolated and will only interact directly with a single anion (or cation). However, very high concentrations require that each water interact with multiple ionic species, since the coordination numbers of the halide anions and of the sodium cation in water are ∼6.[1] No evidence is observed in the XAS data (e.g., nonlinearity) to indicate a change between these two regimes over the measured concentration range. This indicates that very few water molecules form hydrogen bonds with more than a single anion and that the XAS measurements are sensitive primarily to changes in the first solvation shell; thus, ion−ion interactions, even in these relatively concentrated solutions, are negligible. A similar conclusion was recently obtained by Weber et al. for various iodide solutions using photoelectron spectroscopy.[9] This was determined based on the independence of the solvated I$^-$ (4d) binding energy to both concentration and counterion, although a large shift in the I$^-$ binding energy of the solvated anion vs the gas-phase anion was observed.

Comparisons to experimental vibrational Raman spectra of alkali metal halide solutions can also be made. In both the −OH bending and stretching regions, the Raman intensity increases with the addition of chloride and iodide salts, although there is no observation of spectral broadening or new features.[4] The changes in the −OH stretch Raman spectrum upon salt addition are nearly independent of the identity of the halide (for Cl$^-$, Br$^-$, and I$^-$ salts; F$^-$ exhibits markedly different behavior),

although for a given concentration the heavy halides lead to slightly larger spectral changes.[28] It was also found that the major Raman spectral changes in the librational and vibrational regions vary linearly with electrolyte concentration, even up to concentrations near the saturation point,[4,29,30] similar to the observed XAS changes with salt addition. In the vibrational Raman spectrum, the temperature and salt dependences are qualitatively identical (increase of the high-energy, weak HB region and a decrease of the low-energy, strong HB region),[4] in contrast to the behavior of the aqueous solution XAS spectra. However, whereas increasing temperature produces a decrease in the per-molecule scattering intensity, the addition of the larger halides (Cl⁻, Br⁻, I⁻) leads to a strong increase in the per-molecule scattering. These two results (temperature and salt dependence of the Raman and XAS spectra) indicate that perturbation of the electronic structure of the water molecules by ions or by geometric rearrangement is highly correlated with changes in the internal vibrations of the molecules and that any similarity between the temperature and salt dependence of the vibrational Raman may be coincidental.

Conclusions

We have experimentally measured oxygen K-edge X-ray absorption spectra for various sodium halide solutions up to 4 M and demonstrated that the presence of the ions in solution engenders significant changes in the XAS of liquid water. In particular, a linear increase of the preedge and main edge and a decrease of the postedge are observed. A salt-dependent isosbestic point is observed between the main edge and postedge. We suggest that the observed spectral changes primarily result from direct perturbation of the unoccupied orbitals of anion near-neighbor water molecules by the salt ions. In particular, our results indicate that the changes observed at the main edge arise due to direct perturbation of the unoccupied near-neighbor water orbitals and that, by comparison to the liquid water XAS temperature dependence,[10] changes in the pre- and postedges may arise from a combination of both direct electrostatic ion−water interactions and geometric rearrangement of the HB network (although geometric distortions probably only play a minor role). Density functional theory based calculations show that the presence of the anion leads to a general red shift of water XAS transitions from the postedge to the main edge, leading to a transfer of intensity between the two spectral regions, thus explaining the experimental observation of a salt-dependent isosbestic point between the main edge and postedge. We suggest that further study of the perturbing effects associated with cations could yield interesting insights.

References and Notes

(1) Neilson, G. W.; Mason, P. E.; Ramos, S.; Sullivan, D. *Philos. Trans. R. Soc. London, A* **2001**, *359*, 1575.

(2) Leberman, R.; Soper, A. K. *Nature* **1995**, *378*, 364.

(3) Kropman, M. F.; Bakker, H. J. *Chem. Phys. Lett.* **2003**, *370*, 741.

(4) Schultz, J. W.; Hornig, D. F. *J. Phys. Chem.* **1961**, *65*, 2131.

(5) Robertson, W. H.; Johnson, M. A. *Annu. Rev. Phys. Chem.* **2003**, *54*, 173.

(6) Thompson, W. H.; Hynes, J. T. *J. Am. Chem. Soc.* **2000**, *122*, 6278.

(7) Tobias, D. J.; Jungwirth, P.; Parrinello, M. *J. Chem. Phys.* **2001**, *114*, 7036.

(8) Winter, B.; Weber, R.; Widdra, W.; Dittmar, M.; Faubel, M.; Hertel, I. V. *J. Phys. Chem. A* **2004**, *108*, 2625.

(9) Weber, R.; Winter, B.; Schmidt, P. M.; Widdra, W.; Hertel, I. V.; Dittmar, M.; Faubel, M. *J. Phys. Chem. B* **2004**, *108*, 4729.

(10) Smith, J. D.; Cappa, C. D.; Wilson, K. R.; Messer, B. M.; Cohen, R. C.; Saykally, R. J. *Science* **2004**, *306*, 851.

(11) Wilson, K. R.; Cavalleri, M.; Rude, B. S.; Schaller, R. D.; Nilsson, A.; Pettersson, L. G. M.; Goldman, N.; Catalano, T.; Bozek, J. D.; Saykally, R. J. *J. Phys.: Condens. Matter* **2002**, *14*, L221.

(12) Myneni, S.; Luo, Y.; Naslund, L. A.; Cavalleri, M.; Ojamae, L.; Ogasawara, H.; Pelmenschikov, A.; Wernet, P.; Vaterlein, P.; Heske, C.; Hussain, Z.; Pettersson, L. G. M.; Nilsson, A. *J. Phys.: Condens. Matter* **2002**, *14*, L213.

(13) Cavalleri, M.; Ogasawara, H.; Pettersson, L. G. M.; Nilsson, A. *Chem. Phys. Lett.* **2002**, *364*, 363.

(14) Bergmann, U.; Wernet, P.; Glatzel, P.; Cavalleri, M.; Pettersson, L. G. M.; Nilsson, A.; Cramer, S. P. *Phys. Rev. B* **2002**, *6609*, 2107.

(15) Guo, J. H.; Luo, Y.; Augustsson, A.; Rubensson, J. E.; Sathe, C.; Agren, H.; Siegbahn, H.; Nordgren, J. *Phys. Rev. Lett.* **2002**, *8913*, 7402.

(16) Naslund, L. A.; Cavalleri, M.; Ogasawara, H.; Nilsson, A.; Pettersson, L. G. M.; Wernet, P.; Edwards, D. C.; Sandstrom, M.; Myneni, S. *J. Phys. Chem. A* **2003**, *107*, 6869.

(17) Wilson, K. R.; Rude, B. S.; Smith, J.; Cappa, C.; Co, D. T.; Schaller, R. D.; Larsson, M.; Catalano, T.; Saykally, R. J. *Rev. Sci. Instrum.* **2004**, *75*, 725.

(18) Wilson, K. R.; Rude, B. S.; Catalano, T.; Schaller, R. D.; Tobin, J. G.; Co, D. T.; Saykally, R. J. *J. Phys. Chem. B* **2001**, *105*, 3346.

(19) Hermann, K.; Pettersson, L. G. M.; Casida, M. E.; Daul, C.; Goursot, A.; Koester, A.; Proynov, E.; St-Amant, A.; Salahub, D. R.; Carravetta, V.; Duarte, H.; Godbout, N.; Guan, J.; Jamorski, C.; Leboeuf, M.; Malkin, V.; Malkina, O.; Nyberg, M.; Pedocchi, L.; Sim, F.; Triguero, L.; Vela, A. *StoBe-deMon v. 2.0*; StoBe Software, available at http://w3.rz-berlin.mpg.de/~hermann/StoBe/, 2004.

(20) Jungwirth, P.; Tobias, D. J. *J. Phys. Chem. B* **2002**, *106*, 6361.

(21) The broadening scheme used here was selected to provide a reasonable representation of the experimental pure water NEXAFS spectrum.

(22) Triguero, L.; Pettersson, L. G. M.; Agren, H. *Phys. Rev. B* **1998**, *58*, 8097.

(23) Pettersson, L. G. M.; Wahlgren, U.; Gropen, O. *J. Chem. Phys.* **1987**, *86*, 2176.

(24) Cappa, C. D.; Smith, J.; Messer, B. M.; Cohen, R. C.; Saykally, R. J. Unpublished results.

(25) Ohtaki, H.; Radnai, T. *Chem. Rev.* **1993**, *93*, 1157.

(26) Cavalleri, M.; Odelius, M.; Nilsson, A.; Pettersson, L. G. M. *J. Chem. Phys.* **2004**, *121*, 10065.

(27) Wernet, P.; Nordlund, D.; Bergmann, U.; Cavalleri, M.; Odelius, M.; Ogasawara, H.; Naslund, L. A.; Hirsch, T. K.; Ojamae, L.; Glatzel, P.; Pettersson, L. G. M.; Nilsson, A. *Science* **2004**, *304*, 995.

(28) Terpstra, P.; Combes, D.; Zwick, A. *J. Chem. Phys.* **1990**, *92*, 65.

(29) Walrafen, G. E. *J. Chem. Phys.* **1966**, *44*, 1546.

(30) Young, T. F.; Maranville, L. F.; Smith, H. M. In *The structure of electrolytic solutions*; Hamer, W. J., Ed.; John Wiley & Sons: New York, 1959.